Letter

Melanin-like Nanoquencher on Graphitic Carbon Nitride Nanosheets for Tyrosinase Activity and Inhibitor Assay

Jin-Wen Liu, Yu-Min Wang, Liu Xu, Lu-Ying Duan, Hao Tang, Ru-Qin Yu, and Jian-hui Jiang

Anal. Chem., **Just Accepted Manuscript** • DOI: 10.1021/acs.analchem.6b01667 • Publication Date (Web): 15 Jul 2016

Melanin-like Nanoquencher on Graphitic Carbon Nitride Nanosheets for Tyrosinase Activity and Inhibitor Assay

Jin-Wen Liu, Yu-Min Wang, Liu Xu, Lu-Ying Duan, Hao Tang*, Ru-Qin Yu, and Jian-Hui Jiang*

Institute of Chemical Biology and Nanomedicine, State Key Laboratory of Chemo/Bio-Sensing and Chemometrics, College of Chemistry and Chemical Engineering, Hunan University, Changsha 410082 (P. R. China)

Email: haotang@hnu.edu.cn; jianhuijiang@hnu.edu.cn; Tel: 86-731-88821916; Fax : 86-731-88821916

ABSTRACT: Graphitic C_3N_4 (g-C_3N_4) nanosheets are a type of emerging graphene-like carbon-based nanomaterials with high fluorescence and large specific surface areas that hold great potential for biosensor applications. However, current g-C_3N_4 based biosensors have prevailingly limited to coordination with metal ions, and it is of great significance to develop new designs for g-C_3N_4 nanosheets based biosensors toward biomarkers of general interest. We report the development of a novel g-C_3N_4 nanosheet-based nanosensor strategy for highly sensitive, single-step and label-free detection of tyrosinase (TYR) activity and its inhibitor. This strategy relies on the catalytic oxidation of tyrosine by TYR into a melanin-like polymers, which form a nanoassembly on the g-C_3N_4 nanosheets and quench their fluorescence. This strategy was demonstrated to provide excellent selectivity and superior sensitivity and to enable rapid screening for TYR inhibitors. Therefore, the developed approach might create a useful platform for diagnostics and drugs screening for TYR-based diseases including melanoma cancer.

Carbon-based nanostructures such as carbon nanotube, graphene and graphene oxide (GO), fullerene and carbon nanoparticles and dots, represent a class of promising materials for diverse applications.[1,2] The implementation of carbon-based nanostructures for biomedical devices and sensors is of particular significance, because of their excellent water dispersibility in water through simple oxidation, high biocompatibility, and low cytotoxicity as compared with other inorganic nanomaterials.[3,4] Only very few carbon-based nanomaterials have been found to be fluorescent, such as carbon or GO quantum dots.[5-7] Nevertheless, the small size (< 10 nm) increases the difficulty in surface engineering of these superfine nanomaterials.[8] Moreover, this size also limit their efficiency as an intracellular transport carriers.[9,10] Although two-dimensional nanomaterials may have the potential to overcome these issues. These non-fluorescent carbon-based nanostructured sensors are usually developed in virtue of their ability to quench fluorescence, so they typically required adsorption or immobilization with fluorophore-labeled biomolecules.[11-16] Pursuit for fluorescent carbon-based nanomaterials with a high surface-to-volume ratio, easy functionali-zation and controlled size is highly demanding.

Graphitic carbon nitride (g-C_3N_4) nanosheets are a type of emerging graphene-like, carbon-based two-dimensional nanomaterials with high fluorescence quantum yield.[17,18] Compared with the very small fluorescent GO quantum dots, g-C_3N_4 nanosheets can be prepared in varying sizes up to hundreds of nanometers. These sizable nanosheets provide the possibility of tethering a high load of biomolecules on a single nanosheet using varying engineering strategies. Moreover, g-C_3N_4 nanosheets are able to deliver much higher photoluminescence than GO because of their high-degree condensation of the tri-s-triazine unit.[19] These properties make g-C_3N_4 nanosheets a useful platform for biosensor applications. Currently, most of g-C_3N_4nanosheetsbased fluorescent biosensors usually relies on their coordination with metal ions, and these sensors have been demonstrated for detection of Cu^{2+}, Fe^{3+}, Ag^{+}, Cr^{3+}, CN^{-}, ascorbic acid and biothiols.[20-23] It is of great significance to develop new designs for g-C_3N_4 nanosheet based biosensors toward biomarkers of general interest. Given their high surface-to-volume ratio and large π-systems, g-C_3N_4 nanosheets hold the potential for high-affinity and selective interactions with biomacromolecules. Motivated by this hypothesis, we explore to develop a novel biosensor for tyrosinase. Tyrosinase (TYR) is an oxidoreductase that participates in the biosynthesis of melanin. Recent evidences revealed that loss of tyrosinase activity confers increased skin tumor, and the expression levels of tyrosinase are very much elevated in melanoma,[24] suggesting TYR as a useful biomarker for melanoma. Therefore, the development of a simple, rapid, label-free and sensitive method for

monitoring TYR activity and screening its inhibitors is of great interest for diagnostics of melanoma cancer.

Herein we report the development of a novel g-C_3N_4 nanosheet-based nanosensor strategy for highly sensitive, single-step and label-free detection of TYR activity and its inhibitors. This strategy relies on the catalytic oxidation of tyrosine by TYR into melanin-like polymers, which form a nanoassembly with the g-C_3N_4 nanosheets and quench their fluorescence, as shown in Scheme 1. In a mixture of g-C_3N_4 and tyrosine, tyrosine is oxidized in the presence of TYR into L-3, 4-dihydrophenylalanine (L-DOPA) (Scheme S1 in Supporting Information). L-DOPA is then oxidized by dissolved O_2 into corresponding quinone, which undergoes a sequence of redox isomerization and catechol oxidation, eventually yielding melanin-like oligomers.[25] Because of the high surface-to-volume ratio and large π-systems in the g-C_3N_4 nanosheets, the melanin-like oligomers are supposed to easily assemble on the surface, which seeds *in situ* growth of melanin-like polymers on the nanosheets. This reaction results in the formation of a nanoassembly of the melanin-like coating on the g-C_3N_4 nanosheets. Moreover, the as-formed melanin-like coating can act as an energy acceptor efficiently quenching the fluorescence of g-C_3N_4 nanosheets, giving an indicator for the activity of TYR.

Scheme 1. Principle for g-C_3N_4 nanosheets based nanosensor strategy for TYR detection.

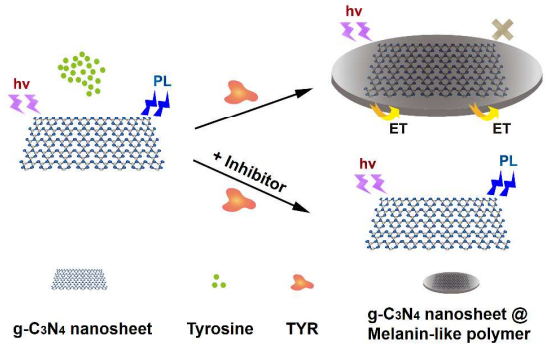

The g-C_3N_4 nanosheets were prepared by chemical oxidation of a bulk g-C_3N_4 material with nitric acid followed by a liquid exfoliating method.[19,26] The bulk g-C_3N_4 material was observed as solid rocky-like agglomerates consisting of irregular folded flakes with approximately several micrometers in size (Figure S1 and S2 in SI). Transmission electron microscope (TEM, Figure 1A) and dynamic light scattering (DLS) showed a mean diameter of 90 to 110 nm for the nanosheets (Figure S3 in SI). Moreover, a positive zeta potential of 25.4 mV was observed for the nanosheets solution, indicating a positive charged surface for the nanosheets which helped to maintain their good dispersibility in water (Figure S4 in SI). Atomic force microscope (AFM) images of the g-C_3N_4 nanosheets showed a thickness ranging from 1.4 nm to 2.3 nm (Figure S5 in SI), indicating that the nanosheets merely comprised one or two layers.[27,28] XRD patterns revealed that the interlayer stacking distance slightly decreased from 0.325 nm to 0.322 nm after exfoliation, indicating that the bulk g-C_3N_4 was successfully exfoliated into nanoscale layered structures (Figures 1B).[17] FT-IR analysis also showed characteristic bands for the nanosheets (Figure S6 in SI). The peak at 811 cm^{-1} was attributed to the vibration of the triazine ring, and the peaks around 1000 and 1800 cm^{-1} were ascribed to the stretching modes of CN heterocycles. XPS measurements revealed three major chemical elements (C, N, O) with a C/N/O ratio of 0.436/0.520/0.044 for the nanosheets (Figure 1C), in which the relatively high oxygen content was commonly obtained for the g-C_3N_4 nanosheets prepared using chemical oxidation and liquid exfoliation. The C1s spectrum gave two peaks at 284.7, and 288.1 eV, which are attributed to graphitic carbon, sp3-bonded carbon with oxygen (C-OH), and sp2-bonded carbon (N–C=N), respectively(Figure 1D). The O1s spectrum displayed two peaks at 531.6 and 532.7 eV, which were attributed to N–C=O and C–OH (Figure 1E). The N1s spectrum showed four peaks at 398.7, 399.8, 401.1 and 404.3 eV, corresponding to sp2-hybridizedaromatic nitrogen bonded to carbon atoms (C=N–C), C-NH bond, quaternary N bonded to three C in the aromatic cycles, and charging effects or positive charge localization inheterocycles (Figure 1F).[19] The g-C_3N_4 nanosheets displayed a broad absorption band with an onset near 300 nm and an intensive blue fluorescence with an excitation peak at 310 nm and an emission maximum at 438 nm(Figure S7 in SI). The quantum yield of the nanosheets was determined to be ~15.6% (Figure S8 in SI). Moreover, their fluorescence was quite stable, and only slight changes were found under continuous illumination for 2 h (Figure S9 in SI). Taken together, these results demonstrated the successful synthesis of the g-C_3N_4 nanosheets.

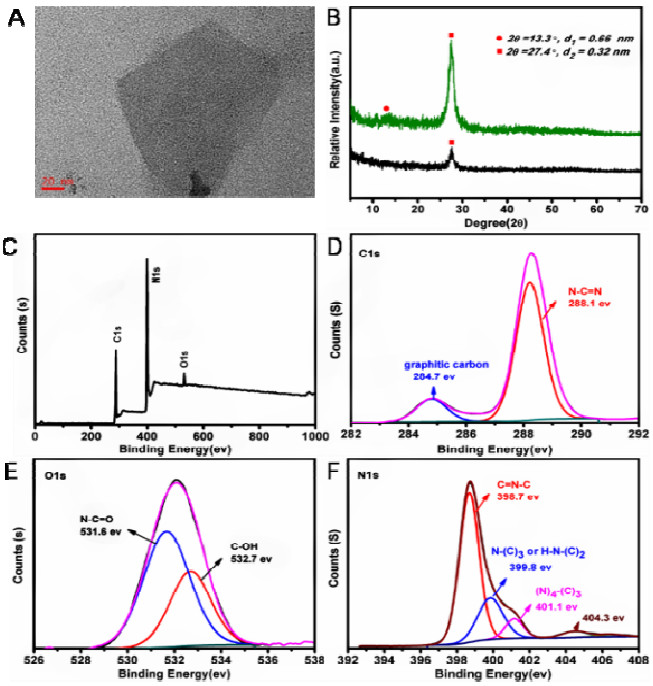

Figure 1. (A) TEM image of the g-C_3N_4 nanosheets. (B) XRD patterns of bulk g-C_3N_4 (green) and g-C_3N_4 nanosheets (black). (C) Survey XPS spectrum of g-C_3N_4 nanosheets. (D) C1s spectrum of g-C_3N_4 nanosheets. (E) O1s spectrum of g-C_3N_4 nanosheets. (F) N1s spectrum of g-C_3N_4 nanosheets.

With the as-prepared nanosheets, we then test their feasibility as a fluorescent sensing platform for TYR detection (Figure 2). When mixed with tyrosine (1 mM), the nanosheets did not exhibit appreciable changes in the fluorescence peak at 438 nm, suggested that tyrosine had little effect on the fluorescence of the nanosheets. In contrast, when 10 μg/mL TYR added in the g-C_3N_4/tyrosine mixture, a remarkable fluorescence decrease (>90%) was obtained. In a control experiment in which tyrosine was absent, no fluorescence quenching appeared. These findings clearly demonstrated that fluorescence quenching of the nanosheets was attributed to a TYR mediated reaction with tyrosine. Presumably, TYR was able to mediate an oxidation reaction with tyrosine in the presence of dissolved O_2, which eventually formed melanin-like polymer strongly adsorbed on the g-C_3N_4nanosheets. Considering the possibility for the melanin-like polymer as an efficient energy receptor,[29] and the absorbance spectrum of melanin-like polymers overlaps well with the emission spectrum of the g-C_3N_4 nanosheets (Figure S10 in SI), fluorescence resonance energy transfer (FRET) between the nanosheets and the melanin-like polymer could induce substantial quenching of the fluorescence for the nanosheets. An additional experiment was performed using bulk g-C_3N_4 instead of the nanosheets, and we found that bulk g-C_3N_4 showed a much lower signal-to-background ratio than the nanosheets (Figure S11 in SI). This finding testified the advantage of g-C_3N_4 nanosheets over bulk materials for biosensor development.

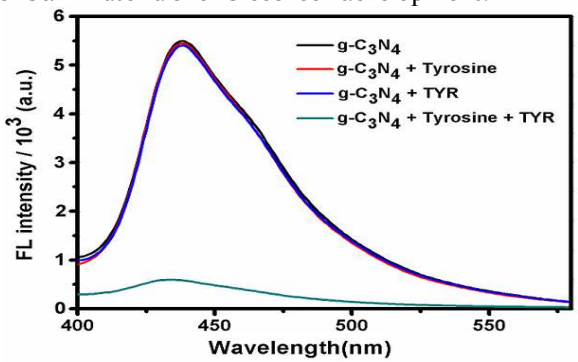

Figure 2. Fluorescence spectral responses obtained from g-C_3N_4 (black); g-C_3N_4+tyrosine (red); g-C_3N_4+TYR (blue); g-C_3N_4+tyrosine+TYR (green). Reactions were performed at 37 °C for 1.0 h and tyrosine 1 mM, TYR 10μg/mL, and 5 μg/mL g-C_3N_4 were used for all experiments.

A closer investigation was performed to understand the mechanism of the sensing strategy. As shown by the AFM images, the g-C_3N_4nanosheets gave a topological height of ~2.3 nm, atypical dimension for two-layered sheets. In contrast, after the TYR reaction, the fluorescence-quenched nanosheets gave a topological height over 10 nm. This finding indicated that there was a coating layer on the g-C_3N_4nanosheets, evidencing the *in situ* formation of a melanin-like polymer on the surface of g-C_3N_4 nanosheets (Figure S12 in SI). A further interrogation with time-resolved fluorescence decay measurements for the g-C_3N_4 nanosheets were performed to shed light on the fluorescence quenching mechanism (Figure S13 in SI). The fluorescence decay curve of the g-C_3N_4nanosheets was fitted using a double exponential function, with τ_1 of 3.3 ns (81.5%) and τ_2 of 16.0 ns (18.5%), respectively, and the average lifetime was 5.65 ns. The average lifetime of the melanin-like polymer coated g-C_3N_4 nanoassembly was decreased to 1.86 ns, with τ_1 of 1.3 ns (88.1%) and τ_2 of 6.0 ns (11.9%), implying a dynamic quenching process with an accelerated FRET-induced deactivation rate for the excited state. Time-dependent measurements of the responses to 5 μg/mL TYR showed a gradually decreased fluorescence signals within 45 min (Figure S14 in SI), indicating a *in situ* growth process of the melanin-like coating on the nanosheets. MALID-TOF/TOF analysis was performed to estimate the molecular weight of the products obtained at different reaction time (Figure S15 in SI). The results indicated only small oligomers ranging from 500 to 1063 Da) were obtained during the reaction, indicating time-dependent fluorescence quenching was ascribed to increasing concentration of small oligomers rather than large ones.

Next, we investigated the ability of the sensing strategy for quantitative assays of TYR. The fluorescence spectral signals for the g-C_3N_4 nanosheets were found to decrease with increasing TYR concentrations (Figure 3). A TYR concentration of 5 μg/mL gave a quenching ratio up to ~9, indicating a high signal-to-background ratio for this assay. A linear correlation was achieved between the peak fluorescence intensities at 438 nm to the logarithmic concentrations of TYR in the range from 1.0 ng/mL to 1.0 μg/mL (Figure S16 in SI). The detection limit was estimated to be as low as 0.6 ng/mL, which at least 50 times better than those for previously reported methods (Table S1 in SI).This result revealed that the developed strategy provided a very sensitive sensing platform for TYR activity.

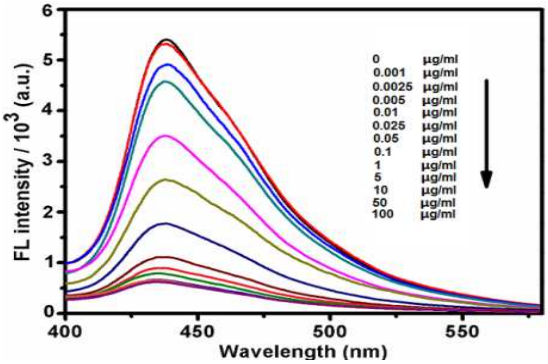

Figure 3. Fluorescence responses of g-C_3N_4 nanosheets with tyrosine to TYR of varying concentrations.

To evaluate the specificity of the assay, we performed the assays with some common potentially interfering

substances (Figure S17 in SI). Assays using other proteins such as bovine serum albumin (BSA), urease, lysozyme, GOx, AChE and complex biological matrices such as fetal bovine serum (10%) and HeLa cell lysate (10^6 cells) all showed little fluorescence quenching. These data confirmed the high selectivity of the sensing strategy and suggested its feasibility for TYR activity and inhibitor detection. To evaluate feasibility for real sample assay, our method was then tested using four serum samples by adding tyrosinase of different concentrations in 10-fold diluted serum. The recoveries were in the range from 94.9% and 102.4% (Table S2 in SI), indicating the potential of the method for real sample analysis.

The developed strategy could also be applied to the screening of inhibitors of TYR. To demonstrate it, we used kojic acid (KA), a potent TYR inhibitor,[30] as the case of study. In the case, TYR was preliminarily incubated with KA of different concentrations for 5 min followed by the reaction in the g-C_3N_4/tyrosine mixture. It was found that the fluorescence intensities increased with increasing KA concentration, clearly indicating the inhibition of TYR activity (Figure S18 in SI). The IC_{50} value (inhibitor concentration producing 50% inhibition) of KA was estimated to be 2.5 μg/mL, which was comparable with the literature value.[31] These results suggested that the proposed method held the potential for quantitative screening of the TYR inhibitors.

In conclusion, we developed a novel fluorescent biosensor strategy that enabled rapid, label-free and sensitive assay for TYR activity and its inhibitors using fluorescent g-C_3N_4 nanosheets. Compare to other carbon-based nanomaterials, g-C_3N_4 nanosheets has many unique advantages including high fluorescence quantum yield and high surface-to-volume ratio. However, the lack of functional groups had limited its utility as a versatile sensing platform. Our sensing strategy provided a paradigm for development of g-C_3N_4 nanosheets based biosensors. This strategy relied on the TYR-mediated *in situ* growth of amelanin-like coating on the fluorescent g-C_3N_4 nanosheets, which induced an efficient FRET-based fluorescence quenching of the nanosheets enabling highly sensitive, single-step and label-free detection of TYR activity. Moreover, this strategy did not require complicated labeling procedure and synthesis of designed substrates. The developed approach was demonstrated to provide excellent selectivity and superior sensitivity and to hold potential in TYR inhibitor screening. This approach can be directly extended to development of biosensors toward peroxidase or its substrates by using its catalytic pigment-forming reactions with phenols or anilines. It can also be generalized to detect supramolecular assembly or its breaking-down reactions between hydrophobic polymers and fluorescence-quenching materials. Therefore, the developed approach might create a useful platform for biosensor development for biomedicine.

ASSOCIATED CONTENT

Supporting Information

Additional detailed information as noted in the text. Experimental details, instrumental parameters, characterization results, method validation results. This material is available free of charge via the Internet at http://pubs.acs.org.

Notes

The authors declare no competing financial interest.

ACKNOWLEDGMENT

This work was supported by NSFC (21527810, 21205034, 21190041, 21521063) and National Key Basic Research Program (2011CB911000).

REFERENCES

(1) Zhang, H. *ACS Nano* **2015,** *9,* 9451-9469.
(2) Zhu, J.; Yang, D.; Yin, Z.; Yan, Q.; Zhang, H. *Small* **2014,** *10,* 3480-3498.
(3) Baptista, F. R.; Belhout, S. A.; Giordani, S.; Quinn, S. J. *Chem. Soc. Rev.* **2015,** *44,* 4433-4453.
(4) Hong, G.; Diao, S.; Antaris, A. L.; Dai, H. *Chem. Rev.* **2015**, *115,* 10816-10906.
(5) Baker, S. N.; Baker, G. A. *Angew. Chem., Int. Ed.* **2010,** *49,* 6726-6744.
(6) Zhu, S.; Meng, Q.; Wang, L.; Zhang, J.; Song, Y.; Jin, H.; Zhang, K.; Sun, H.; Wang, H.; Yang, B. *Angew. Chem., Int. Ed.* **2013,** *52,* 3953-3957.
(7) Lim, S. Y.; Shen, W.; Gao, Z. *Chem. Soc. Rev.* **2015,** *44,* 362-381.
(8) Huang, X.; Zeng, Z.; Bao, S.; Wang, M.; Qi, X.; Fan, Z.; Zhang, H. *Nat. Commun.* **2013,** *4,* 1444.
(9) Jiang, W.; Kim, B. Y. S.; Rutka, J. T.; Chan, W. C. W. *Nat. Nanotech.* **2008,** *3,* 145-150.
(10) Sun, T.; Zhang, Y. S.; Pang, B.; Hyun, D. C.; Yang, M.; Xia, Y. *Angew. Chem., Int. Ed.* **2014,** *53,* 12320-12364.
(11) Lu, C. H.; Yang, H. H.; Zhu, C. L.; Chen, X.; Chen, G. N. *Angew. Chem., Int. Ed.* **2009,** *48,* 4785-4787.
(12) Chen, T. T.; Tian, X.; Liu, C.L.; Ge, J.; Chu, X.; Li, Y. *J. Am. Chem. Soc.* **2015,** *137,* 982-989.
(13) Zhu, C.; Zeng, Z.; Li, H.; Li, F.; Fan, C.; Zhang, H. *J. Am. Chem. Soc.* **2013,** *135,* 5998-6001.
(14) Zhang, Y.; Zheng, B.; Zhu, C.; Zhang, X.; Tan, C.; Li, H.; Chen, B.; Yang, J.; Chen, J.; Huang, Y.; Wang, L.; Zhang, H. *Adv. Mater.* **2015,** *27,* 935-939.
(15) Tan, C. Yu, P.; Hu, Y.; Chen, J.; Huang, Y.; Cai, Y.; Luo, Z.; Li, B.; Lu, Q.; Wang, L.; Liu, Z.; Zhang, H. *J. Am. Chem. Soc.* **2015,** *137,* 10430-10436.
(16) Zhao, M.; Wang, Y.; Ma, Q.; Huang, Y.; Zhang, X.; Ping, J.; Zhang, Z.; Lu, Q.; Yu, Y.; Xu, H.; Zhao, Y.; Zhang, H. *Adv. Mater.* **2015,** *27,* 7372-7378.
(17) Zhang, X.; Xie, X.; Wang, H.; Zhang, J.; Pan, B.; Xie, Y. *J. Am. Chem. Soc.* **2013,** *135,* 18-21.
(18) Zhang, X. L.; Zheng, C.; Guo, S. S.; Li, J.; Yang, H. H.; Chen, G. *Anal. Chem.* **2014,** *86,* 3426-3434.
(19) Rong, M.; Lin, L.; Song, X.; Zhao, T.; Zhong, Y.; Yan, J.; Wang, Y.; Chen, X. *Anal. Chem.* **2015,** *87,* 1288-1296.
(20) Lee, E. Z.; Jun, Y. S.; Hong, W. H.; Thomas, A.; Jin, M. M. *Angew. Chem., Int. Ed.* **2010**, *49,* 9706-9710.
(21) Lee, E. Z.; Lee, S. U.; Heo, N. S.; Stucky, G. D.; Jun, Y. S.; Hong, W. H. *Chem. Commun.* **2012,** *48,* 3942-3944.
(22) Tian, J.; Liu, Q.; Asiri, A. M.; Al-Youbi, A. O.; Sun, X. *Anal. Chem.* **2013,** *85,* 5595-5599.
(23) Tang, Y.; Song, H.; Su, Y.; Lv, Y. *Anal. Chem.* **2013,** *85,* 11876-11884.
(24) Angeletti, C.; Khomitch, V.; Halaban, R.; Rimm, D. L. *Diagn. Cytopathol.* **2004,** *31,* 33-37.

(25) d'Ischia, M.; Napolitano, A.; Ball, V.; Chen, C. T.; Buehler, M. J. *Acc. Chem. Res.* **2014,** *47,* 3541-3550.
(26) Wang, X.; Maeda, K.; Thomas, A.; Takanabe, K.; Xin, G.; Carlsson, J. M.; Domen, K.; Antonietti, M. *Nat. Mater.* **2009,** *8,* 76-80.
(27) Wang, X.; Maeda, K.; Chen, X.; Takanabe, K.; Domen, K.; Hou, Y.; Fu, X.; Antonietti, M. *J. Am. Chem. Soc.* **2009,** *131,* 1680-1681.
(28) Xiang, M. H.; Liu, J. W.; Li, N.; Tang, H.; Yu, R. Q.; Jiang, J. H. *Nanoscale* **2016,** *8,* 4727-4732.
(29) Fan, Q.; Cheng, K.; Hu, X.; Ma, X.; Zhang, R.; Yang, M.; Lu, X.; Xing, L.; Huang, W.; Gambhir, S. S.; Cheng, Z. *J. Am. Chem. Soc.* **2014,** *136,* 15185-15194.
(30) Chang, T. S. *Int. J. Mol. Sci.* **2009,** *10,* 2440-2475.
(31) Chen, Z.; Cai, D.; Mou, D.; Yan, Q.; Sun, Y.; Pan, W.; Wan, Y.; Song, H.; Yi, W. *Bioorg. Med. Chem.* **2014,** *22,* 3279-3284.

Table of Contents (TOC)